

**Bose-Einstein correlations in $K^\pm K^\pm$ pairs
from Z^0 decays into two hadronic jets**

The OPAL collaboration

Abstract

Bose-Einstein correlations in pairs of charged kaons produced in a sample of 3.9 million hadronic Z^0 decays have been measured with the OPAL experiment at LEP. Charged kaons were identified in the central tracking detector using their specific energy loss in the drift chamber gas. The correlation function was studied in two-jet events using a double ratio, formed by the number of like-sign pairs normalised by a reference sample in the data, divided by the same ratio in a Monte Carlo simulation. The enhancement at small values of the four-momentum difference of the pair was parametrised using a Gaussian function. The parameters of the Bose-Einstein correlations were measured to be $\lambda = 0.82 \pm 0.22 \pm_{0.12}^{0.17}$ for the strength and $R_0 = 0.56 \pm 0.08 \pm_{0.06}^{0.08}$ fm for the kaon source radius, where the first errors are statistical and the second systematic. Corrections for final-state interactions are discussed.

(Submitted to European Physical Journal C)

The OPAL Collaboration

G. Abbiendi², K. Ackerstaff⁸, P.F. Akesson³, G. Alexander²³, J. Allison¹⁶,
K.J. Anderson⁹, S. Arcelli¹⁷, S. Asai²⁴, S.F. Ashby¹, D. Axen²⁹, G. Azuelos^{18,a},
I. Bailey²⁸, A.H. Ball⁸, E. Barberio⁸, R.J. Barlow¹⁶, J.R. Batley⁵, S. Baumann³,
T. Behnke²⁷, K.W. Bell²⁰, G. Bella²³, A. Bellerive⁹, S. Bentvelsen⁸, S. Bethke^{14,i},
S. Betts¹⁵, O. Biebel^{14,i}, A. Biguzzi⁵, I.J. Bloodworth¹, P. Bock¹¹, J. Böhme^{14,h},
O. Boeriu¹⁰, D. Bonacorsi², M. Boutemeur³³, S. Braibant⁸, P. Bright-Thomas¹,
L. Brigliadori², R.M. Brown²⁰, H.J. Burckhart⁸, P. Capiluppi², R.K. Carnegie⁶,
A.A. Carter¹³, J.R. Carter⁵, C.Y. Chang¹⁷, D.G. Charlton^{1,b}, D. Chrisman⁴,
C. Ciocca², P.E.L. Clarke¹⁵, E. Clay¹⁵, I. Cohen²³, J.E. Conboy¹⁵, O.C. Cooke⁸,
J. Couchman¹⁵, C. Couyoumtzelis¹³, R.L. Coxe⁹, M. Cuffiani², S. Dado²²,
G.M. Dallavalle², S. Dallison¹⁶, R. Davis³⁰, A. de Roeck⁸, P. Dervan¹⁵,
K. Desch²⁷, B. Dienes^{32,h}, M.S. Dixit⁷, M. Donkers⁶, J. Dubbert³³, E. Duchovni²⁶,
G. Duceck³³, I.P. Duerdoth¹⁶, P.G. Estabrooks⁶, E. Etzion²³, F. Fabbri²,
A. Fanfani², M. Fanti², A.A. Faust³⁰, L. Feld¹⁰, P. Ferrari¹², F. Fiedler²⁷,
M. Fierro², I. Fleck¹⁰, A. Frey⁸, A. Fürtjes⁸, D.I. Futyan¹⁶, P. Gagnon¹²,
J.W. Gary⁴, G. Gaycken²⁷, C. Geich-Gimbel³, G. Giacomelli², P. Giacomelli²,
D.M. Gingrich^{30,a}, D. Glenzinski⁹, J. Goldberg²², W. Gorn⁴, C. Grandi²,
K. Graham²⁸, E. Gross²⁶, J. Grunhaus²³, M. Gruwé²⁷, C. Hajdu³¹, G.G. Hanson¹²,
M. Hansroul⁸, M. Hapke¹³, K. Harder²⁷, A. Harel²², C.K. Hargrove⁷,
M. Harin-Dirac⁴, M. Hauschild⁸, C.M. Hawkes¹, R. Hawkings²⁷,
R.J. Hemingway⁶, G. Herten¹⁰, R.D. Heuer²⁷, M.D. Hildreth⁸, J.C. Hill⁵,
P.R. Hobson²⁵, A. Hocker⁹, K. Hoffman⁸, R.J. Homer¹, A.K. Honma⁸,
D. Horváth^{31,c}, K.R. Hossain³⁰, R. Howard²⁹, P. Hüntemeyer²⁷, P. Igo-Kemenes¹¹,
D.C. Imrie²⁵, K. Ishii²⁴, F.R. Jacob²⁰, A. Jawahery¹⁷, H. Jeremie¹⁸, M. Jimack¹,
C.R. Jones⁵, P. Jovanovic¹, T.R. Junk⁶, N. Kanaya²⁴, J. Kanzaki²⁴,
G. Karapetian¹⁸, D. Karlen⁶, V. Kartvelishvili¹⁶, K. Kawagoe²⁴, T. Kawamoto²⁴,
P.I. Kayal³⁰, R.K. Keeler²⁸, R.G. Kellogg¹⁷, B.W. Kennedy²⁰, D.H. Kim¹⁹,
A. Klier²⁶, T. Kobayashi²⁴, M. Kobel³, T.P. Kokott³, M. Kolrep¹⁰,
S. Komamiya²⁴, R.V. Kowalewski²⁸, T. Kress⁴, P. Krieger⁶, J. von Krogh¹¹,
T. Kuhl³, M. Kupper²⁶, P. Kyberd¹³, G.D. Lafferty¹⁶, H. Landsman²²,
D. Lanske¹⁴, J. Lauber¹⁵, I. Lawson²⁸, J.G. Layter⁴, D. Lellouch²⁶, J. Letts¹²,
L. Levinson²⁶, R. Liebisch¹¹, J. Lillich¹⁰, B. List⁸, C. Littlewood⁵, A.W. Lloyd¹,
S.L. Lloyd¹³, F.K. Loebinger¹⁶, G.D. Long²⁸, M.J. Losty⁷, J. Lu²⁹, J. Ludwig¹⁰,
A. Macchiolo¹⁸, A. Macpherson³⁰, W. Mader³, M. Mannelli⁸, S. Marcellini²,
T.E. Marchant¹⁶, A.J. Martin¹³, J.P. Martin¹⁸, G. Martinez¹⁷, T. Mashimo²⁴,
P. Mättig²⁶, W.J. McDonald³⁰, J. McKenna²⁹, E.A. Mckigney¹⁵, T.J. McMahon¹,
R.A. McPherson²⁸, F. Meijers⁸, P. Mendez-Lorenzo³³, F.S. Merritt⁹, H. Mes⁷,
I. Meyer⁵, A. Michelini², S. Mihara²⁴, G. Mikenberg²⁶, D.J. Miller¹⁵, W. Mohr¹⁰,
A. Montanari², T. Mori²⁴, K. Nagai⁸, I. Nakamura²⁴, H.A. Neal^{12,f}, R. Nisius⁸,
S.W. O’Neale¹, F.G. Oakham⁷, F. Odorici², H.O. Ogren¹², A. Okpara¹¹,
M.J. Oreglia⁹, S. Orito²⁴, G. Pásztor³¹, J.R. Pater¹⁶, G.N. Patrick²⁰, J. Patt¹⁰,

R. Perez-Ochoa⁸, S. Petzold²⁷, P. Pfeifenschneider¹⁴, J.E. Pilcher⁹, J. Pinfold³⁰,
D.E. Plane⁸, B. Poli², J. Polok⁸, M. Przybycień^{8,d}, A. Quadt⁸, C. Rembser⁸,
H. Rick⁸, S.A. Robins²², N. Rodning³⁰, J.M. Roney²⁸, S. Rosati³, K. Roscoe¹⁶,
A.M. Rossi², Y. Rozen²², K. Runge¹⁰, O. Runolfsson⁸, D.R. Rust¹², K. Sachs¹⁰,
T. Saeki²⁴, O. Sahr³³, W.M. Sang²⁵, E.K.G. Sarkisyan²³, C. Sbarra²⁸,
A.D. Schaile³³, O. Schaile³³, P. Scharff-Hansen⁸, J. Schieck¹¹, S. Schmitt¹¹,
A. Schönig⁸, M. Schröder⁸, M. Schumacher³, C. Schwick⁸, W.G. Scott²⁰,
R. Seuster^{14,h}, T.G. Shears⁸, B.C. Shen⁴, C.H. Shepherd-Themistocleous⁵,
P. Sherwood¹⁵, G.P. Siroli², A. Skuja¹⁷, A.M. Smith⁸, G.A. Snow¹⁷, R. Sobie²⁸,
S. Söldner-Rembold^{10,e}, S. Spagnolo²⁰, M. Sproston²⁰, A. Stahl³, K. Stephens¹⁶,
K. Stoll¹⁰, D. Strom¹⁹, R. Ströhmer³³, B. Surrow⁸, S.D. Talbot¹, P. Taras¹⁸,
S. Tarem²², R. Teuscher⁹, M. Thiergen¹⁰, J. Thomas¹⁵, M.A. Thomson⁸,
E. Torrence⁸, S. Towers⁶, T. Trefzger³³, I. Trigger¹⁸, Z. Trócsányi^{32,g}, E. Tsur²³,
M.F. Turner-Watson¹, I. Ueda²⁴, R. Van Kooten¹², P. Vannerem¹⁰,
M. Verzocchi⁸, H. Voss³, F. Wäckerle¹⁰, D. Waller⁶, C.P. Ward⁵, D.R. Ward⁵,
P.M. Watkins¹, A.T. Watson¹, N.K. Watson¹, P.S. Wells⁸, T. Wengler⁸,
N. Vermes³, D. Wetterling¹¹, J.S. White⁶, G.W. Wilson¹⁶, J.A. Wilson¹,
T.R. Wyatt¹⁶, S. Yamashita²⁴, V. Zacek¹⁸, D. Zer-Zion⁸

¹School of Physics and Astronomy, University of Birmingham, Birmingham B15 2TT, UK

²Dipartimento di Fisica dell' Università di Bologna and INFN, I-40126 Bologna, Italy

³Physikalisches Institut, Universität Bonn, D-53115 Bonn, Germany

⁴Department of Physics, University of California, Riverside CA 92521, USA

⁵Cavendish Laboratory, Cambridge CB3 0HE, UK

⁶Ottawa-Carleton Institute for Physics, Department of Physics, Carleton University, Ottawa, Ontario K1S 5B6, Canada

⁷Centre for Research in Particle Physics, Carleton University, Ottawa, Ontario K1S 5B6, Canada

⁸CERN, European Organisation for Particle Physics, CH-1211 Geneva 23, Switzerland

⁹Enrico Fermi Institute and Department of Physics, University of Chicago, Chicago IL 60637, USA

¹⁰Fakultät für Physik, Albert Ludwigs Universität, D-79104 Freiburg, Germany

¹¹Physikalisches Institut, Universität Heidelberg, D-69120 Heidelberg, Germany

¹²Indiana University, Department of Physics, Swain Hall West 117, Bloomington IN 47405, USA

¹³Queen Mary and Westfield College, University of London, London E1 4NS, UK

¹⁴Technische Hochschule Aachen, III Physikalisches Institut, Sommerfeldstrasse 26-28, D-52056 Aachen, Germany

¹⁵University College London, London WC1E 6BT, UK

¹⁶Department of Physics, Schuster Laboratory, The University, Manchester M13 9PL, UK

¹⁷Department of Physics, University of Maryland, College Park, MD 20742, USA

¹⁸Laboratoire de Physique Nucléaire, Université de Montréal, Montréal, Quebec H3C 3J7, Canada

¹⁹University of Oregon, Department of Physics, Eugene OR 97403, USA

²⁰CLRC Rutherford Appleton Laboratory, Chilton, Didcot, Oxfordshire OX11 0QX, UK

²²Department of Physics, Technion-Israel Institute of Technology, Haifa 32000, Israel

²³Department of Physics and Astronomy, Tel Aviv University, Tel Aviv 69978, Israel

²⁴International Centre for Elementary Particle Physics and Department of Physics, University of Tokyo, Tokyo 113-0033, and Kobe University, Kobe 657-8501, Japan

²⁵Institute of Physical and Environmental Sciences, Brunel University, Uxbridge, Middlesex UB8 3PH, UK

²⁶Particle Physics Department, Weizmann Institute of Science, Rehovot 76100, Israel

²⁷Universität Hamburg/DESY, II Institut für Experimental Physik, Notkestrasse 85, D-22607 Hamburg, Germany

²⁸University of Victoria, Department of Physics, P O Box 3055, Victoria BC V8W 3P6, Canada

²⁹University of British Columbia, Department of Physics, Vancouver BC V6T 1Z1, Canada

³⁰University of Alberta, Department of Physics, Edmonton AB T6G 2J1, Canada

³¹Research Institute for Particle and Nuclear Physics, H-1525 Budapest, P O Box 49, Hungary

³²Institute of Nuclear Research, H-4001 Debrecen, P O Box 51, Hungary

³³Ludwigs-Maximilians-Universität München, Sektion Physik, Am Coulombwall 1, D-85748 Garching, Germany

^a and at TRIUMF, Vancouver, Canada V6T 2A3

^b and Royal Society University Research Fellow

^c and Institute of Nuclear Research, Debrecen, Hungary

^d and University of Mining and Metallurgy, Cracow

^e and Heisenberg Fellow

^f now at Yale University, Dept of Physics, New Haven, USA

^g and Department of Experimental Physics, Lajos Kossuth University, Debrecen, Hungary

^h and MPI München

ⁱ now at MPI für Physik, 80805 München.

1 Introduction

Intensity interferometry was applied in 1953 by Hanbury-Brown and Twiss [1] in radio astronomy in order to estimate the spatial extension of stars (HBT effect). In particle reactions which lead to multi-hadronic final states the HBT effect manifests itself as a constructive interference between two identical bosons — the so-called Bose-Einstein (BE) correlation, which is now well known and was first observed by Goldhaber et al. [2] in $\bar{p}p$ annihilations. There is interest in the quantum mechanical aspects of the BE correlations, but they are also used to estimate the dimensions of the source of the identical bosons. BE correlation studies of pion pairs have been carried out in a large variety of particle interactions and over a wide range of energies [3–5]. Recently, pion BE correlations have been investigated in connection with the W mass measurement in $e^+e^- \rightarrow W^+W^-$ reactions at LEP at centre-of-mass energies above 161 GeV [6, 7].

Compared to the abundant information now available on BE correlations in pion pairs, knowledge of the correlations in identical strange boson pairs is scarce and, until recently, was mainly limited to the $K_s^0 K_s^0$ system. $K_s^0 K_s^0$ pairs may exhibit a BE correlation enhancement near threshold even if the origin is not a $K^0 K^0$ or $\bar{K}^0 \bar{K}^0$ system but a $K^0 \bar{K}^0$ boson-antiboson system. A $K_s^0 K_s^0$ low-mass enhancement has recently been observed in hadronic Z^0 decays [8–11]. However, the interpretation of this enhancement as a pure BE correlation effect is complicated by the possible presence of the $f_0(980)$ decay into $K^0 \bar{K}^0$. Recently it has been pointed out that the information from BE correlation studies of the $K^\pm K^\pm$ system, which cannot result from the $f_0(980)$ decay, can serve as an effective tool in setting a limit on the resonant fraction of the $K_s^0 K_s^0$ BE enhancement [12].

The study of $K^\pm K^\pm$ BE correlations also has a bearing on the relation between the dimension of the emitting source and the mass of the emitted particles; from recent measurements it has been pointed out that the source dimension seems to decrease as the mass increases [13]. Several models have been proposed to account for this behaviour [13, 14].

This paper presents a study of $K^\pm K^\pm$ BE correlations using the high statistics sample of Z^0 hadronic events recorded by the OPAL detector at LEP. The paper is organised as follows. In Section 2 the methodology used for measuring the BE correlations is presented. The event and track selections are described in Section 3. In Section 4 the analysis of the data is presented, and in Section 5 the systematic effects are studied. Finally, the conclusions are drawn in Section 6.

2 Analysis method

The BE correlation function for two identical bosons is defined as:

$$C(p_1, p_2) = \frac{\rho(p_1, p_2)}{\rho(p_1)\rho(p_2)}, \quad (1)$$

where $\rho(p_1, p_2) = (1/\sigma)(d^8\sigma/d^4p_1d^4p_2)$ is the two-particle phase space density subject to BE symmetry, and $\rho(p)$ is the corresponding single particle quantity for a particle with four-momentum p . The correlation function can be studied as a function of the four-momentum difference of the pair, Q , where $Q^2 = -(p_1 - p_2)^2 = M^2 - 4m_{\text{boson}}^2$, and M is the invariant mass of the pair of bosons each of mass m_{boson} .

From the study of the correlation in pairs one can determine the geometrical and dynamical properties of the emitting source. For a static sphere of emitters with Gaussian density, the correlation function is parametrised with the Goldhaber function [3] as:

$$C(Q) = 1 + \lambda e^{-(RQ)^2}, \quad (2)$$

where λ , the strength of the correlation, is 0 for a completely coherent source and 1 for a completely incoherent one. The parameter R in GeV^{-1} is related to the radius of the source, R_0 , through the relation $R_0 = R\hbar c$.

The two-particle phase space density $\rho(p_1, p_2)$ is obtained from a sample of pairs of identical bosons. In this analysis this sample, called the like-sign sample, is formed by pairs of kaons with the same charge. The denominator of Equation 1 $\rho(p_1)\rho(p_2)$ is in practice replaced by a reference distribution $\rho_0(p_1, p_2)$, which resembles $\rho(p_1, p_2)$ in all aspects except in the BE symmetry. A perfect reference sample should have the following properties: absence of BE correlations, and presence of the same correlations as in the the like-sign sample, arising from energy-momentum and charge conservation, the topology and global properties of the events, and resonance or long-lived particle decays.

The principal difficulty for measurements of BE correlations is in the definition of the reference sample from which $\rho_0(p_1, p_2)$ is obtained. When correlations amongst like-sign boson pairs are measured, the obvious reference sample is provided by unlike-sign boson pairs. Unfortunately, the Q distribution of the unlike-sign pairs includes prominent peaks due to neutral meson resonances (e.g. $\phi \rightarrow K^+K^-$). An alternative reference sample can be derived from Monte Carlo simulations in which BE correlations are not included. This relies on a correct simulation of the physics in the complete absence of any BE effect, and a correct modeling of detector effects. A third type of reference sample can be obtained using the methods of event- or hemisphere-mixing, where particles from different events or hemispheres are combined. The last, least model-dependent method was used in the present work.

Each event was divided into two hemispheres separated by the plane perpendicular to the thrust axis and containing the interaction point. A charged kaon track in one hemisphere was combined with a kaon track of the same charge found in the opposite hemisphere after reflecting the momentum of this second track through the origin. To ensure that the like-sign and reference samples were independent, the two kaon tracks forming a pair in the like-sign sample were required

to be in the same hemisphere. If all the events have two back-to-back jets, the reference sample of hemisphere-mixed pairs will be similar to the like-sign pair sample apart from the lack of BE correlations. Monte Carlo studies have shown that the hemisphere-mixing technique only works in symmetric topologies such as back-to-back jets. Therefore, two-jet events were selected by requiring a high value of the thrust. The event- and hemisphere-mixing techniques have already been used in other experiments [15, 16].

3 Event and track selection

A detailed description of the OPAL detector can be found in reference [17]. This analysis is primarily based on information from the central tracking detectors, consisting of a silicon microvertex detector, a vertex drift chamber, a jet chamber and z -chambers¹, all of which lie within an axial magnetic field of 0.435 T. The jet chamber, which has an outer radius of 185 cm, provides up to 159 measurements of space points per track with a resolution in the r - ϕ plane of about 135 μm and a transverse momentum² resolution of $\sigma_{p_T}/p_T = \sqrt{(0.02)^2 + (0.0015 p_T)^2}$, with p_T in GeV/c . Particle identification in the jet chamber is possible using the measurement of the specific energy loss dE/dx [18] with a resolution of approximately of 3% for high-momentum tracks in hadronic decays [19]. Since the identification of charged kaons using dE/dx is crucial to this analysis, the calibration of the energy loss over the many years of data taking was checked and improved when necessary. Control samples of particles identified by techniques other than the energy loss were used to remove year-to-year variations in the measured dE/dx and to resolve discrepancies between the measured dE/dx in the data and the theoretical dE/dx in the Monte Carlo.

This analysis used a sample of about 3.9 million hadronic Z^0 decays recorded at LEP between the years 1992 and 1995. A sample of 6.75 million Monte Carlo hadronic events generated with JETSET 7.4 [20] and tuned to reproduce the global features of the events [21] was also used. The generated events were processed through a detailed simulation of the experiment [22] and subjected to the same event and track selection as the data. A detailed description of the selection of hadronic events is given in [23]. Events with two clear back-to-back jets, necessary for the proper functioning of the hemisphere-mixing technique, were selected by requiring that the thrust value was larger than 0.95. About 30% of the events passed the thrust cut.

Charged tracks were required to have a minimum transverse momentum of 150 MeV/c , a maximum reconstructed momentum of 60 GeV/c , a distance of

¹A right handed coordinate system is used, with positive z along the e^- beam direction and x pointing towards the centre of the LEP ring. The polar and azimuthal angles are denoted by θ and ϕ , and the origin is taken to be the centre of the detector.

²The projection onto the plane perpendicular to the beam axis.

closest approach to the interaction point less than 0.5 cm in the plane orthogonal to the beam direction and the corresponding distance along the beam direction of less than 40 cm. The first measured point had to be within a radius of 75 cm from the interaction vertex. The cuts on the transverse and longitudinal distances of closest approach help to remove particles from long-lived decays. About 50% of the reconstructed tracks passed these selections.

Kaons were identified using the dE/dx measurement. Only tracks with at least 20 hits available for the measurement of dE/dx and with a polar angle satisfying $|\cos\theta| < 0.9$ were considered. For each track, a χ^2 probability was formed for each stable particle hypothesis: e, μ , π , K and p. A track was identified as a kaon candidate if it had a probability of at least 10% of being a kaon and if the probability of being a kaon was larger than the probability of being any other of the above particle species. In addition, in order to reject pions, each track was required to have a pion probability less than 5%. Electrons from photon conversions were rejected using a neural network algorithm as described in [24]. According to the Monte Carlo, approximately 34% of the true kaons passed these requirements and the estimated kaon purity of the track sample was about 72% on average, with variations between 50% and 97% depending on the momentum of the track. The lowest purity corresponded to the momentum range between 0.9 and 1.5 GeV/ c where the pion and kaon bands overlap in dE/dx [19]. In the selected kaon track sample the fraction of pions was estimated as 17%, that of protons as 11%, and the contribution of muons and electrons was negligible.

4 Data analysis

The Q distributions of the like-sign kaon candidate pairs and the hemisphere-mixed kaon candidate pairs were determined using tracks that passed the selections described in Section 3. In the data, 76063 like-sign and 98558 hemisphere-mixed kaon candidate pairs with $Q < 2.0$ GeV were selected. In the Monte Carlo, the corresponding numbers of kaon candidate pairs were 109601 and 136785 respectively.

Since the BE correlation manifests itself only for identical particles, it was necessary to correct for impurities. The Monte Carlo predicted that the main contamination in the sample of like-sign kaon candidate pairs was from $K\pi$ and Kp pairs. In this sample, and for pairs with $Q < 2.0$ GeV, the estimated fraction of KK pairs was about 48%, the $K\pi$ fraction about 27% and the Kp fraction about 13%. The contamination from pairs susceptible to BE correlations or Fermi-Dirac anti-correlations (i.e. $\pi\pi$ and pp) was negligible, of the order of 3% for $\pi\pi$ and less than 1% for pp pairs. The fraction of KK pairs was constant over the whole Q range. The sample of hemisphere-mixed kaon candidate pairs had an almost identical composition.

The Monte Carlo non-KK Q distribution was subtracted from the data distri-

bution using the fraction given by the simulation and normalised to the number of data pairs. Both like-sign and hemisphere-mixed pair distributions were corrected using this technique. Figure 1 shows these corrected Q distributions for the data and the Monte Carlo in which BE correlations were not simulated. The hemisphere-mixed Q distributions were normalised to the like-sign Q distributions in the region $0.6 < Q < 2.0$ GeV where no BE correlations are expected. Both data and Monte Carlo distributions show a similar behaviour at high values of Q : the hemisphere-mixed distribution is above the like-sign one in the region $0.7 < Q < 1.2$ GeV; there is a cross-over of both distributions at Q about 1.2 GeV; and the like-sign distribution is above the hemisphere-mixed one at $Q > 1.2$ GeV.

Figure 2 shows the ratio $N_{++}(Q)/N_{mix}(Q)$ in both the data and the Monte Carlo, where $N_{++}(Q)$ is the number of like-sign pairs and $N_{mix}(Q)$ is the number of hemisphere-mixed pairs as functions of Q . The first two bins of the distribution shown in the figure were combined due to the small statistics. The data distribution shows a clear enhancement in the region $Q < 0.3$ GeV. There is also a rise of the correlation at high values of Q normally attributed to long-range correlations. Indeed, the slope of the correlations at high Q is well reproduced by the Monte Carlo. The ratio $N_{++}(Q)/N_{mix}(Q)$ in the Monte Carlo deviates slightly from unity at high Q and falls slowly with decreasing Q , probably due to features of string fragmentation and local conservation of charge and strangeness. These effects can be taken into account if both like-sign and hemisphere-mixed data distributions are divided by the corresponding Monte Carlo distributions.

The correlation function was therefore defined as the double-ratio:

$$C_{mix}(Q) = \frac{N_{++}^{data}(Q)}{N_{mix}^{data}(Q)} / \frac{N_{++}^{MC}(Q)}{N_{mix}^{MC}(Q)}, \quad (3)$$

and was parametrised using a modified version of Equation 2:

$$C(Q) = N (1 + \lambda e^{-(RQ)^2}) (1 + \delta Q + \epsilon Q^2), \quad (4)$$

where N is a normalisation factor, and the empirical term $(1 + \delta Q + \epsilon Q^2)$ accounts for the behaviour of the correlation function at high Q values due to any remaining long-range correlations. Figure 3 shows the correlation $C_{mix}(Q)$ with the result of the fit. The fitted parameters and the correlation coefficients between them are given in Table 1. The fit has a $\chi^2 = 43$ for 35 degrees of freedom.

5 Systematic effects

Systematic effects arising from the event and track selections, the modeling of dE/dx in the Monte Carlo, the parametrisation of the correlation function and the choice of the reference sample are considered. In each case, the result of the

		Correlation coefficients				
	fitted value	N	λ	R_0	δ	ϵ
N	0.97 ± 0.11		-0.59	+0.52	-0.96	+0.85
λ	0.82 ± 0.22			+0.17	+0.58	-0.52
R_0 (fm)	0.56 ± 0.08				-0.42	+0.29
δ (GeV ⁻¹)	-0.07 ± 0.16					-0.96
ϵ (GeV ⁻²)	0.06 ± 0.06					

Table 1: Fitted parameters and correlation coefficients obtained in the Gaussian parametrisation of the correlation function $C_{mix}(Q)$. The uncertainties on the parameters are statistical only.

fit to the correlation function is given in Table 2, with row (a) giving the result of the basic fit discussed in the previous section.

The overall systematic uncertainties in the parameters λ and R_0 were calculated as the largest single deviations between the parameters of the fits from rows (b) to (l), and the parameters of the basic fit in row (a). The final values of the parameters are

$$\begin{aligned}\lambda &= 0.82 \pm 0.22 \begin{matrix} +0.17 \\ -0.12 \end{matrix} \\ R_0 &= 0.56 \pm 0.08 \begin{matrix} +0.08 \\ -0.06 \end{matrix} \text{ fm.}\end{aligned}$$

The mismodeling of the kaon momentum spectrum, residual BE correlations in the reference sample, the origins of the kaons and final-state interaction corrections are also discussed in this section.

5.1 Event and track selection

- As discussed in Section 2, the hemisphere-mixing technique only works when two-jet events are selected. The analysis was repeated for events selected using a cone jet finding algorithm [25] instead of the cut in thrust (row (b)). The value of the thrust cut was also changed from 0.95 to 0.93 and the analysis repeated (row (c)).
- To obtain a purer sample of kaons, tracks with momenta in the pion-kaon dE/dx overlap region, $0.9 < p < 1.5$ GeV/ c , were rejected (row (d)).
- The minimum number of dE/dx hits required for each track was increased from 20 to 40 (row (e)).

5.2 Parametrisation of dE/dx

Since the analysis relies to a large extent on the separation of pions from kaons, it is especially important to understand the dE/dx measurements of the copiously-produced pions. A sample of pions was identified in $K_s^0 \rightarrow \pi^+\pi^-$ decays [8]

and was used to estimate the mismodeling of the normalised ionisation energy loss $N_{dE/dx}^\sigma$ [24]. The normalised dE/dx is defined as $N_{dE/dx}^\sigma = (dE/dx - (dE/dx)_0)/(\sigma(dE/dx))_0$. Here, dE/dx is the measured value, while $(dE/dx)_0$ and $(\sigma(dE/dx))_0$ are the expected value and the expected error assuming the track to be a pion. This analysis showed that the mean value and the width of the normalised dE/dx distribution were both known to within $\pm 10\%$ of σ . By changing in the Monte Carlo the normalised dE/dx of both kaons and pions by their known uncertainties, the fraction of non-KK pairs was found to vary by up to $\pm 10\%$. The BE analysis was consequently repeated with the assumed impurity value set to 57% and 47% (rows (f) and (f')).

5.3 Fit of the correlation function

- The binning of the Q distributions was modified from 50 MeV to 20 MeV (row (g)).
- The Q distribution normalisation range was changed from $0.6 < Q < 2.0$ GeV to $0.8 < Q < 2.0$ GeV (row (h)).
- The fit was repeated with the first bin $Q < 0.05$ GeV, excluded. This was done to test the effect of potential problems at low Q because of the limited resolution [26] (row (i)).
- If the use of the double-ratio removes all correlations other than BE, such as long-range correlations at high Q , then the empirical term $(1 + \delta Q + \epsilon Q^2)$ of Equation 4 would not be necessary. $C_{mix}(Q)$ was parametrised using the simplified function:

$$C(Q) = N(1 + \lambda e^{-(RQ)^2}). \quad (5)$$

The parameters of the fit are given in row (j). The fit has $\chi^2 = 49$ for 37 degrees of freedom. This fit was also repeated with the range limited to $Q < 1.5$ GeV to reduce possible long-range correlations (row (k)).

5.4 The reference sample

The BE correlation was also measured using Monte Carlo like-sign pairs as the reference sample in the sub-sample of two-jet events (row (l)). The correlation function in this case was defined as:

$$C_{MC}(Q) = \frac{N_{++}^{data}(Q)}{N_{++}^{MC}(Q)}. \quad (6)$$

Figure 4 shows the correlation function $C_{MC}(Q)$ together with the results of a fit using Equation 4. The values of the parameters are: $N = 0.88 \pm 0.05$; $\lambda = 0.92$

± 0.17 ; $R_0 = 0.59 \pm 0.06$ fm; $\delta = 0.04 \pm 0.08$ GeV $^{-1}$; $\epsilon = 0.05 \pm 0.03$ GeV $^{-2}$, where the errors are statistical only. The fit has $\chi^2 = 42$ for 35 degrees of freedom.

Although there are known imperfections in the simulation, particularly at low momenta in the kaon momentum spectrum (see section 5.5), these results were taken as an indication of systematic differences between the hemisphere-mixing method and the simple use of a Monte Carlo reference sample.

fit variation	λ	R_0 (fm)	χ^2/DoF
(a) basic fit	0.82 ± 0.22	0.56 ± 0.08	43/35
(b) cone jet finding	0.90 ± 0.21	0.58 ± 0.13	45/35
(c) thrust > 0.93	0.88 ± 0.19	0.53 ± 0.06	42/35
(d) cut on p	0.89 ± 0.23	0.58 ± 0.08	37/35
(e) minimum $N_{dE/dx} = 40$	0.79 ± 0.27	0.62 ± 0.13	43/35
(f) $dE/dx + 10\%$	0.99 ± 0.26	0.55 ± 0.07	44/35
(f') $dE/dx - 10\%$	0.70 ± 0.20	0.58 ± 0.11	42/35
(g) Q binning of 20 MeV	0.77 ± 0.22	0.50 ± 0.06	80/95
(h) normalisation $0.8 < Q < 2.0$ GeV	0.82 ± 0.21	0.56 ± 0.08	43/35
(i) Q lower limit 0.05 GeV	0.82 ± 0.23	0.57 ± 0.09	43/34
(j) fit using Equation 5	0.85 ± 0.21	0.64 ± 0.08	49/37
(k) Q upper limit 1.5 GeV	0.81 ± 0.21	0.59 ± 0.08	38/28
(l) Monte Carlo as reference sample	0.92 ± 0.17	0.59 ± 0.06	42/35
Overall systematic error	+ 0.17	+ 0.08	
	- 0.12	- 0.06	

Table 2: Results of various fits of the BE correlation function; the quoted errors associated with λ and R_0 are statistical only. The results in row (a) correspond to the basic fit of Section 4 while the other lines show the results obtained when modifying certain criteria as explained in the text. The overall systematic uncertainties in the parameters λ and R_0 were calculated as the largest single deviations between the parameters of the fits from rows (b) to (l), and the parameters of the basic fit in row (a). The final systematic uncertainties in λ and R_0 are given in the last row.

5.5 Mismodeling of the kaon momentum spectrum

If the simulation were perfect, one would expect to get the same results by measuring the correlation function with $C_{mix}(Q)$ and with $C_{MC}(Q)$. The double-ratio

$$C_{mix}(Q) = \frac{N_{++}^{data}(Q)}{N_{mix}^{data}(Q)} / \frac{N_{++}^{MC}(Q)}{N_{mix}^{MC}(Q)} \equiv \frac{N_{++}^{data}(Q)}{N_{++}^{MC}(Q)} / \frac{N_{mix}^{data}(Q)}{N_{mix}^{MC}(Q)} \quad (7)$$

is equivalent to $C_{MC}(Q)$ only if the hemisphere-mixed sample is perfectly modelled, which implies $N_{mix}^{data}(Q)/N_{mix}^{MC}(Q) = 1$. Figure 5 shows this ratio; the general agreement is good, although at $Q < 0.8$ GeV there is some indication that the ratio is below unity.

Any important mismodeling of the Monte Carlo would indicate that the results obtained with $C_{MC}(Q)$ and with $C_{mix}(Q)$ (since the Monte Carlo is used for normalising this correlation function) were not reliable. Therefore, the distribution of Monte Carlo tracks in a sample free from BE correlations was compared to the same distribution in the data. Figure 6 shows the momentum spectrum of kaon candidate tracks of the hemisphere-mixed sample in the data and in the Monte Carlo normalised to the same total number of pairs. At low momentum, the Monte Carlo does not describe the data spectrum well and differences are seen at the $\pm 15\%$ level. Studies of the differential cross-section of kaons in hadronic events in both the data and the Monte Carlo events, generated with JETSET 7.4 and tuned according to OPAL data, showed that the simulation predicted a kaon spectrum which is too soft.

As a check of the stability of the results obtained with $C_{mix}(Q)$, the Q spectra of both like-sign and hemisphere-mixed pairs were reweighted. Each pair of kaons in the Monte Carlo was reweighted by the product of the weights of each kaon in the pair, where the weight was obtained in bins of momentum by dividing the data momentum spectrum by the Monte Carlo spectrum. The final measurement of the correlation function did not change significantly after reweighting, λ varied by $+0.03$ and R_0 by -0.01 fm. The same exercise was done to check the results obtained with $C_{MC}(Q)$. In this case, λ varied more significantly, by $+0.12$, and R_0 by -0.01 fm. Thus, by the use of a double-ratio technique, the correlation function $C_{mix}(Q)$ was found to be less sensitive to the Monte Carlo mismodeling than the correlation function $C_{MC}(Q)$.

5.6 Residual BE correlations in the reference sample

As suggested in [15], residual BE correlations could be a source of imperfection in the reference sample. To check that the hemisphere-mixed sample was free of effects induced by the BE correlations, a Monte Carlo study was done using the generator JETSET 7.4. Hadronic events were generated with and without BE correlations, with the BE correlations simulated assuming the Goldhaber parametrisation described in Section 2. The shape of the Q distribution of the hemisphere-mixed pairs remained unchanged after including the BE correlations in the generation. The ratio $N_{mix}^{with\ BE}(Q)/N_{mix}^{without\ BE}(Q)$ was consistent with unity in the full range of Q , demonstrating that the reference sample was free from effects due to residual BE correlations.

5.7 Sources of kaons

In a substantial fraction of the kaon pairs, one or more of the kaons result from a long-lived particle decay — in such cases the kaon pairs cannot exhibit BE correlations. It is therefore useful to separate the various sources of kaons and to classify the parent particles to estimate the maximum possible value of λ , as suggested in [4]. On the other hand, some studies [27–29] have suggested that the correlation function is narrowed by the contribution of decay products of long-lived sources, and also that resonance decays induce a pair-momentum dependence of the radius.

The kaon sources as predicted by the JETSET Monte Carlo simulation are given in Table 3. These have been classified as in [4, 27] into two main groups: long-lived sources with life-time $c\tau > 10$ fm, and short-lived sources with life-time $c\tau < 10$ fm. The table shows that the fraction of kaon pairs at low Q (< 0.6 GeV) with at least one kaon from a short-lived source is about 81%, so that the fraction of pairs in which both kaons arise from short-lived sources is about 66%.

The pairs from short-lived sources cannot be identified in the data, and so the final results of this analysis were not corrected for the effect of short-lived sources because such a correction would be based on a Monte Carlo model with its inherent uncertainties. However, to illustrate the magnitude of the effect, a correction was applied to the correlation function using the estimated fraction of short-lived sources (66%), assuming that kaons from long-lived sources do not contribute to the correlations. The fitted parameters of the corrected correlation function are: $\lambda = 1.27 \pm 0.31$ and $R_0 = 0.55 \pm 0.07$ fm, where the errors are statistical only.

	origin of kaons	fraction of kaons in pairs with $Q < 0.6$ GeV
long-lived sources	b, c hadron decays	12%
life-time $c\tau > 10$ fm	$\phi(1020)$	7%
short-lived sources	string fragmentation	40%
life-time $c\tau < 10$ fm	$f_0(980)$	1%
	$K^*(892)$	27%
	other sources	13%

Table 3: Origins of kaons in like-sign pairs with low Q in the Monte Carlo.

5.8 Final-state interactions

Charged kaons are subject to both the Coulomb and the strong interactions. In principle, every pair of like-sign kaons from short-lived sources should be corrected for these interactions in the data (but not in the Monte Carlo, where they were not simulated). To apply a correction to all pairs would result in an overestimate

of the value of the strength parameter [30]. As in Section 5.7, the final results of this analysis were not corrected for the electromagnetic and strong interactions because of the model-dependence of such corrections.

As a check of the possible magnitude of any correction, the electromagnetic repulsion of like-sign pairs was corrected for in the data. The like-sign kaon pair Q spectrum was corrected using the Gamow factor [31] $G(\eta) = 2\pi\eta/(e^{2\pi\eta} - 1)$, where $\eta = \alpha_{em} m_K/Q$, α_{em} is the electromagnetic coupling constant and m_K the kaon mass. On the assumption that all pairs are from short-lived sources, the fitted strength and radius of the Coulomb corrected correlation function are: $\lambda = 0.92 \pm 0.25$ and $R_0 = 0.61 \pm 0.17$ fm, where the errors are statistical only. The correlation function was also corrected for both the effect of short-lived sources as in Section 5.7 and the Coulomb effect, resulting in the fitted parameters: $\lambda = 1.36 \pm 0.55$ and $R_0 = 0.58 \pm 0.11$ fm, where the errors are statistical only.

6 Discussion and conclusions

Bose-Einstein correlations have been measured in identified pairs of charged kaons in hadronic Z^0 decays using the OPAL experiment at LEP. The analysis was performed in events with a clear two-jet topology, a requirement which was necessary to obtain a suitable reference sample using a hemisphere-mixing technique. Monte Carlo simulation was used to correct for imperfections in the reference sample by use of a double-ratio for the correlation function. The enhancement was parametrised using a Gaussian formula, resulting in a strength

$$\lambda = 0.82 \pm 0.22 \begin{matrix} + 0.17 \\ - 0.12 \end{matrix}$$

and a kaon emitter radius

$$R_0 = 0.56 \pm 0.08 \begin{matrix} + 0.08 \\ - 0.06 \end{matrix} \text{ fm.}$$

A definite conclusion from the present analysis is a confirmation of the results of reference [11], that there are indeed BE correlations in $K^\pm K^\pm$ pairs from hadronic Z^0 decays. This implies that there should be such correlations in $K_s^0 K_s^0$ pairs [12]; therefore it is unlikely that the previously observed threshold enhancements [8–11] can be attributed entirely to the $f_0(980)$ decay into kaons.

Values of λ and R_0 , as measured in hadronic Z^0 decays at LEP for various particle types, are listed for comparison in Table 4. Since there is evidence [26] that λ and R_0 may depend on the event topology, the table gives the type of event used in the various measurements. The reference sample types used in each analysis are also listed: these may be event- or hemisphere-mixed, unlike-sign or Monte Carlo pairs.

In all events and for correlations measured using the unlike-sign reference sample, the radius of charged pion emitters varies between 0.8 and 1.0 fm while

pair	λ		R_0 (fm)		ref. sample	events	experiment
	(stat.)	(sys.)	(stat.)	(sys.)			
$K^\pm K^\pm$	0.82 ± 0.22	${}^{+0.17}_{-0.12}$	0.56 ± 0.08	${}^{+0.08}_{-0.06}$	mixed †	two-jet	this analysis
	0.82 ± 0.11	± 0.25	0.48 ± 0.04	± 0.07	unlike	all	DELPHI [11]
$K_s^0 K_s^0$	1.14 ± 0.23	± 0.32	0.76 ± 0.10	± 0.11	MC	all	OPAL [8]
	0.96 ± 0.21	± 0.40	0.65 ± 0.07	± 0.15	MC	all	ALEPH [9]
	0.61 ± 0.16	± 0.16	0.55 ± 0.08	± 0.12	MC	all	DELPHI [11]
$\pi^\pm \pi^\pm$	0.67 ± 0.01	± 0.02	0.96 ± 0.01	± 0.02	unlike	all	OPAL [26]
	0.65 ± 0.02	—	0.91 ± 0.01	—	unlike	two-jet	OPAL [26]
	0.40 ± 0.02	— ‡	0.49 ± 0.02	—	mixed †	two-jet	ALEPH [15]
	0.62 ± 0.04	— ‡	0.81 ± 0.04	—	unlike †	two-jet	ALEPH [15]
	0.35 ± 0.04	— ‡	0.42 ± 0.04	—	mixed †	two-jet	DELPHI [16]
	0.45 ± 0.02	— ‡	0.82 ± 0.03	—	unlike †	all	DELPHI [16]

Table 4: Summary of the parameters λ and R_0 measured at LEP using the Gaussian parametrisation and for different types of identical pairs. The results marked with † were obtained using the double-ratio technique for the correlation function. All the $\pi^\pm \pi^\pm$ results were corrected for Coulomb interactions and the ones marked with ‡ were in addition corrected for non-pion impurities. The uncertainties are statistical and systematic as labelled.

the radius of the charged kaon emitters is 0.48 ± 0.08 fm. This gives the relation $R_0(\pi^\pm \pi^\pm) > R_0(K^\pm K^\pm)$ — a mass dependence of the emitting source, as already pointed out in [13, 14]. In two-jet events, the measured radius of charged pion emitters is seen to vary between 0.4 and 0.9 fm, inconsistent within the quoted errors. This large variation is usually attributed to the choice of the reference sample: in the case of the unlike-sign reference sample the radius is about 0.8–0.9 fm; in the case of the mixed reference sample the radius is about 0.4–0.5 fm. The comparison of results obtained using the event- or hemisphere-mixing techniques and a double-ratio for the correlation function shows that the present measurement of the radius of the kaon source, 0.56 ± 0.11 fm, is compatible with the previous measurements of the radius of pion sources and does not support a strong mass dependence of the emitting source. However, both measurements of R_0 for kaon pairs are considerably larger than that obtained for $\Lambda\Lambda$ pairs, $0.14^{+0.07}_{-0.03}$ fm [13, 32].

Acknowledgements:

We particularly wish to thank the SL Division for the efficient operation of the LEP accelerator at all energies and for their continuing close cooperation with our experimental group. We thank our colleagues from CEA, DAPNIA/SPP, CE-Saclay for their efforts over the years on the time-of-flight and trigger systems which we continue to use. In addition to the support staff at our own institutions we are pleased to acknowledge the
Department of Energy, USA,
National Science Foundation, USA,
Particle Physics and Astronomy Research Council, UK,
Natural Sciences and Engineering Research Council, Canada,
Israel Science Foundation, administered by the Israel Academy of Science and Humanities,
Minerva Gesellschaft,
Benozziyo Center for High Energy Physics,
Japanese Ministry of Education, Science and Culture (the Monbusho) and a grant under the Monbusho International Science Research Program,
Japanese Society for the Promotion of Science (JSPS),
German Israeli Bi-national Science Foundation (GIF),
Bundesministerium für Bildung, Wissenschaft, Forschung und Technologie, Germany,
National Research Council of Canada,
Research Corporation, USA,
Hungarian Foundation for Scientific Research, OTKA T-029328, T023793 and OTKA F-023259.

References

- [1] R. Hanbury-Brown and R.Q. Twiss, *Phil. Mag.* **45** (1954) 663; *Nature* **178** (1956) 1046 and 1447.
- [2] G. Goldhaber, S. Goldhaber, W.B. Fowler, T.F. Hoang, T.E. Kalogeropoulos and W.M. Powell, *Phys. Rev. Lett.* **3** (1959) 181;
G. Goldhaber, S. Goldhaber, W. Lee and A. Pais, *Phys. Rev.* **120** (1960) 300.
- [3] G. Goldhaber, *Proc. Workshop on Local Equilibrium in Strong Interaction Physics (LESIP 1)*, Bad Honnef, Germany (1984), eds. D.K. Scott and R.M. Weiner (World Scientific, Singapore, 1985) p. 155.
- [4] S. Haywood, Rutherford Appleton Laboratory RAL-94-074 (1994).
- [5] E.A. De Wolf, *Proc. XXVII Int. Conf. on High-Energy Physics. Glasgow, U.K. (1994)*, eds. P.J. Bussey and I.G. Knowles (IOP-Publishing, Bristol, 1995) p. 1281.
- [6] OPAL Collaboration, G. Abbiendi *et al.*, CERN-EP/98-174, accepted by *Eur. Phys. J. C*.
- [7] DELPHI Collaboration, P. Abreu *et al.*, *Phys. Lett.* **B401** (1997) 181.
- [8] OPAL Collaboration, R. Akers *et al.*, *Z. Phys.* **C67** (1995) 389.
- [9] ALEPH Collaboration, D. Buskulic *et al.*, *Z. Phys.* **C64** (1994) 361.
- [10] DELPHI Collaboration, P. Abreu *et al.*, *Phys. Lett.* **B323** (1994) 242.
- [11] DELPHI Collaboration, P. Abreu *et al.*, *Phys. Lett.* **B379** (1996) 330.
- [12] G. Alexander and H.J. Lipkin, *Phys. Lett.* **B456** (1999) 270.
- [13] G. Alexander, I. Cohen and E. Levin, *Phys. Lett.* **B452** (1999) 159.
- [14] A. Bialas and K. Zalewski, *Acta Phys. Polon.* **B30** (1999) 359.
- [15] ALEPH Collaboration, D. Decamp *et al.*, *Z. Phys.* **C54** (1992) 75.
- [16] DELPHI Collaboration, P. Abreu *et al.*, *Phys. Lett.* **B286** (1992) 201.
- [17] OPAL Collaboration, K. Ahmet *et al.*, *Nucl. Instr. Meth.* **A305** (1991) 275;
P.P. Allport *et al.*, *Nucl. Instr. Meth.* **A324** (1993) 34.
- [18] M. Hauschild *et al.*, *Nucl. Instr. Meth.* **A314** (1992) 74.
- [19] M. Hauschild, *Nucl. Instr. Meth.* **A379** (1996) 436.

- [20] T. Sjöstrand, *Comp. Phys. Comm.* **82** (1994) 74.
- [21] OPAL Collaboration, G. Alexander *et al.*, *Z. Phys.* **C69** (1996) 543.
- [22] J. Allison *et al.*, *Nucl. Instr. Meth.* **A317** (1992) 47.
- [23] OPAL Collaboration, G. Alexander *et al.*, *Z. Phys.* **C52** (1991) 175.
- [24] OPAL Collaboration, G. Abbiendi *et al.*, *Eur. Phys. J.* **C8** (1999) 217.
- [25] OPAL Collaboration, R. Akers *et al.*, *Z. Phys.* **C63** (1994) 197.
- [26] OPAL Collaboration, G. Alexander *et al.*, *Z. Phys.* **C72** (1996) 389.
- [27] K. Geiger *et al.*, CERN-TH/98-345, submitted to *Phys. Rev.* **D**.
- [28] U.A. Wiedemann and U. Heinz, *Phys. Rev.* **C56** (1997) 610.
- [29] J. Bolz *et al.*, *Phys. Lett.* **B300** (1993) 404; *Phys. Rev.* **D47** (1993) 3860.
- [30] M.G. Bowler, *Phys. Lett.* **B270** (1991) 69.
- [31] M. Gyulassy *et al.*, *Phys. Rev.* **C20** (1979) 2267.
- [32] OPAL Collaboration, G. Alexander *et al.*, *Phys. Lett.* **B384** (1996) 377.

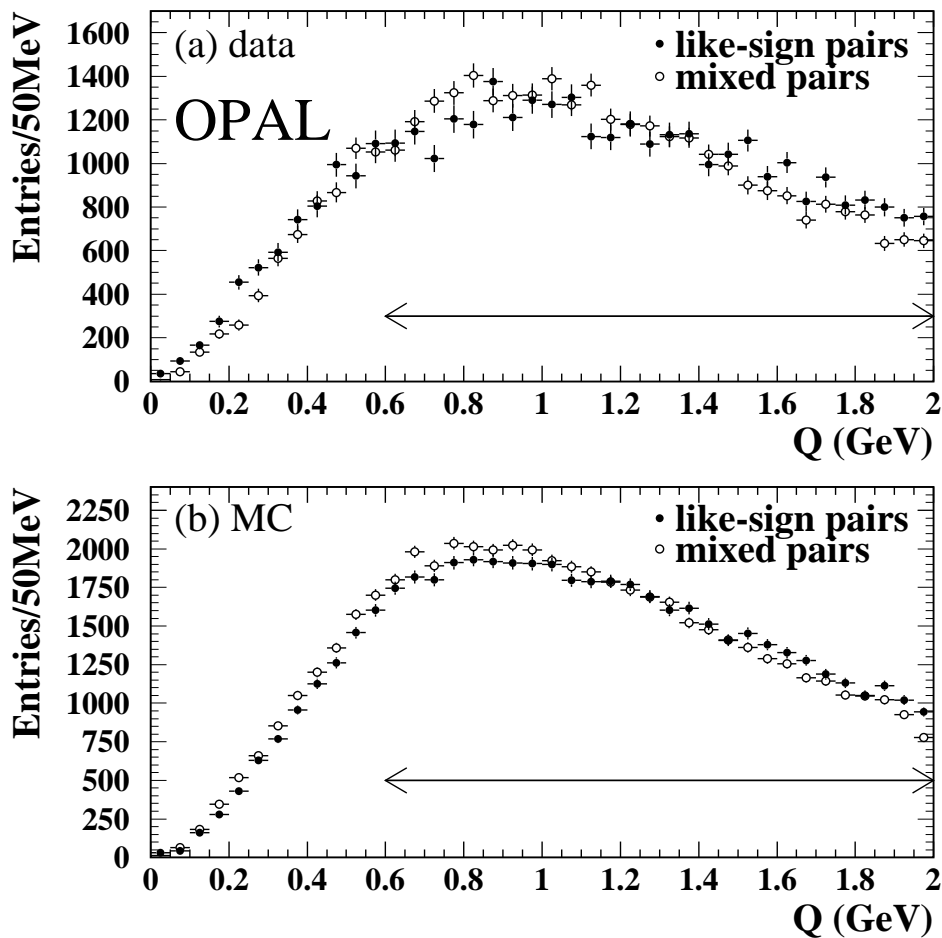


Figure 1: Q distributions of like-sign and hemisphere-mixed KK pairs in the data (a) and in the Monte Carlo without simulation of BE correlations (b). The distributions were corrected for non-KK impurities. The hemisphere-mixed distributions were normalised to the like-sign distributions in the region $0.6 < Q < 2.0$ GeV, indicated by the arrows, where no BE correlations are expected. The errors are statistical only.

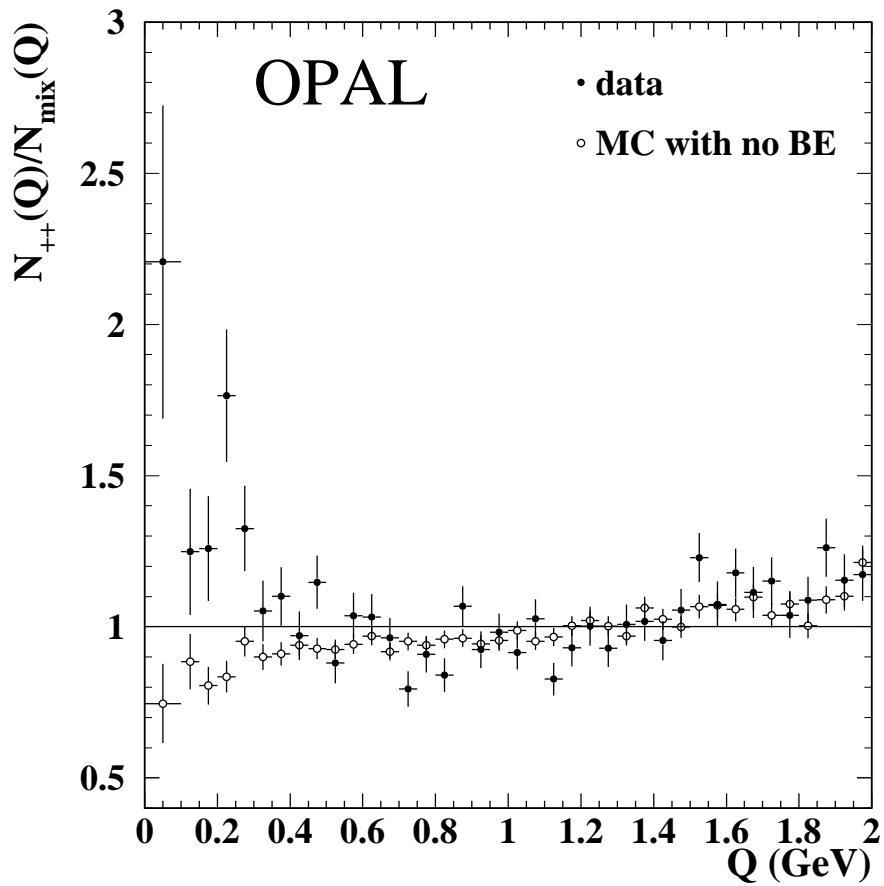


Figure 2: Ratio $N_{++}(Q)/N_{mix}(Q)$ for KK pairs in the data and the Monte Carlo. The first bin has double width due to the small statistics. The errors are statistical only.

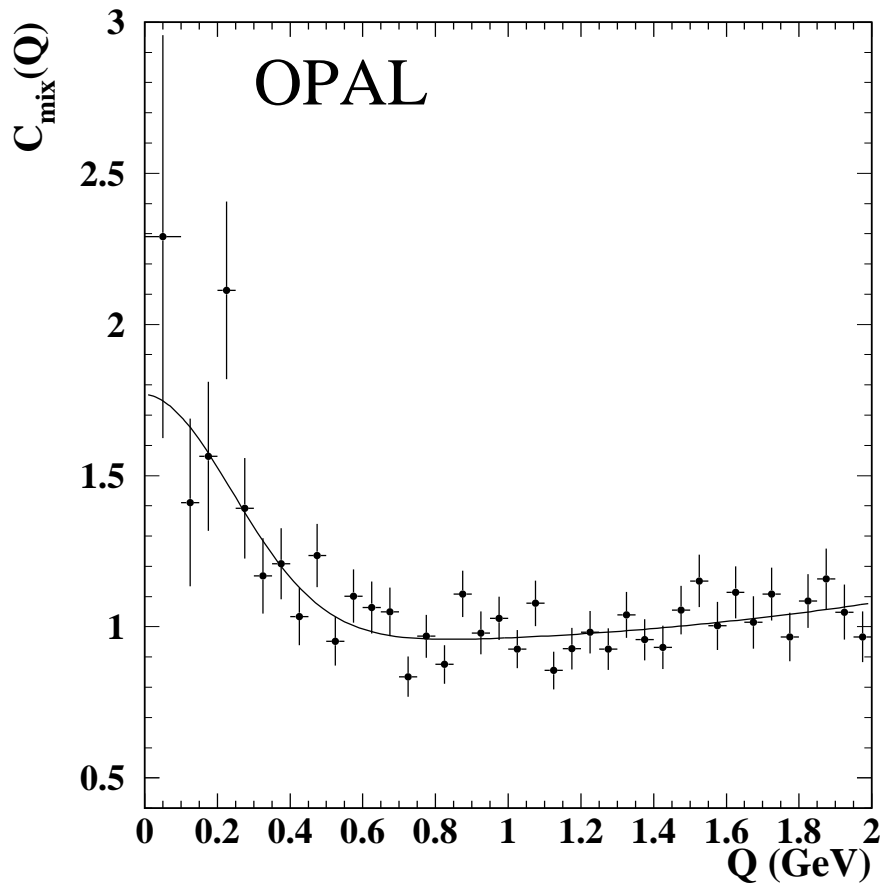


Figure 3: $C_{\text{mix}}(Q)$ BE correlation function in K^+K^+ pairs and the fit using Equation 4 superimposed. The first bin has double width due to the small statistics. The errors are statistical only.

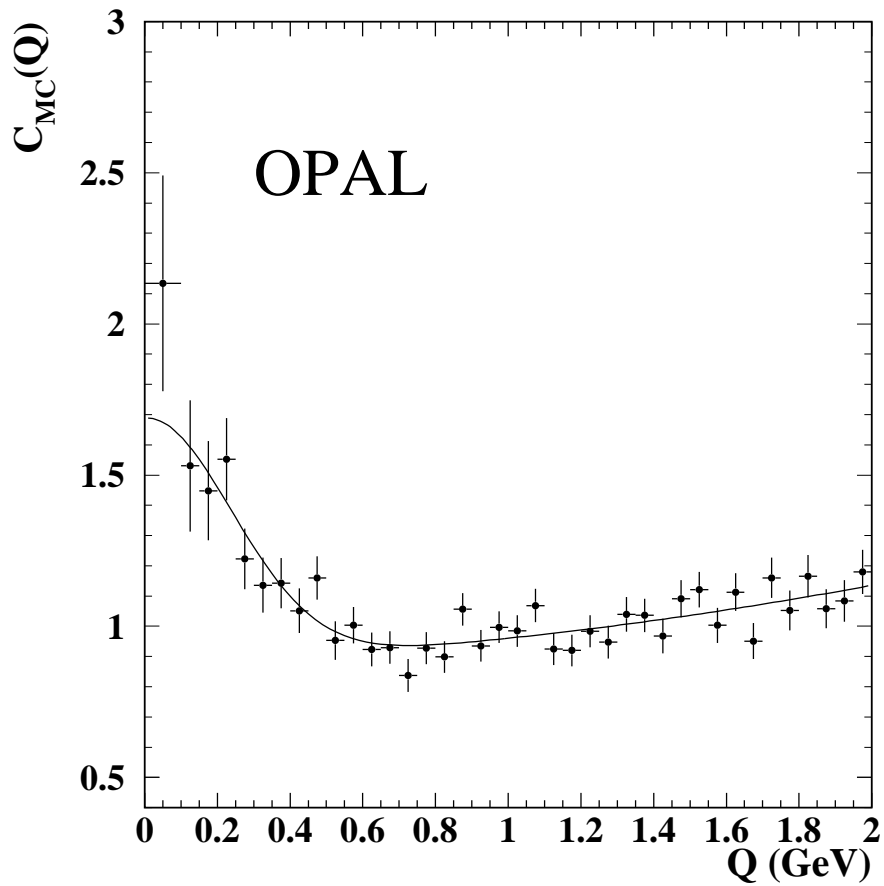


Figure 4: $C_{MC}(Q)$ BE correlation function in $K^\pm K^\pm$ pairs using Monte Carlo like-sign pairs as the reference sample and the fit using Equation 4 superimposed. The first bin has double width due to the small statistics. The errors are statistical only.

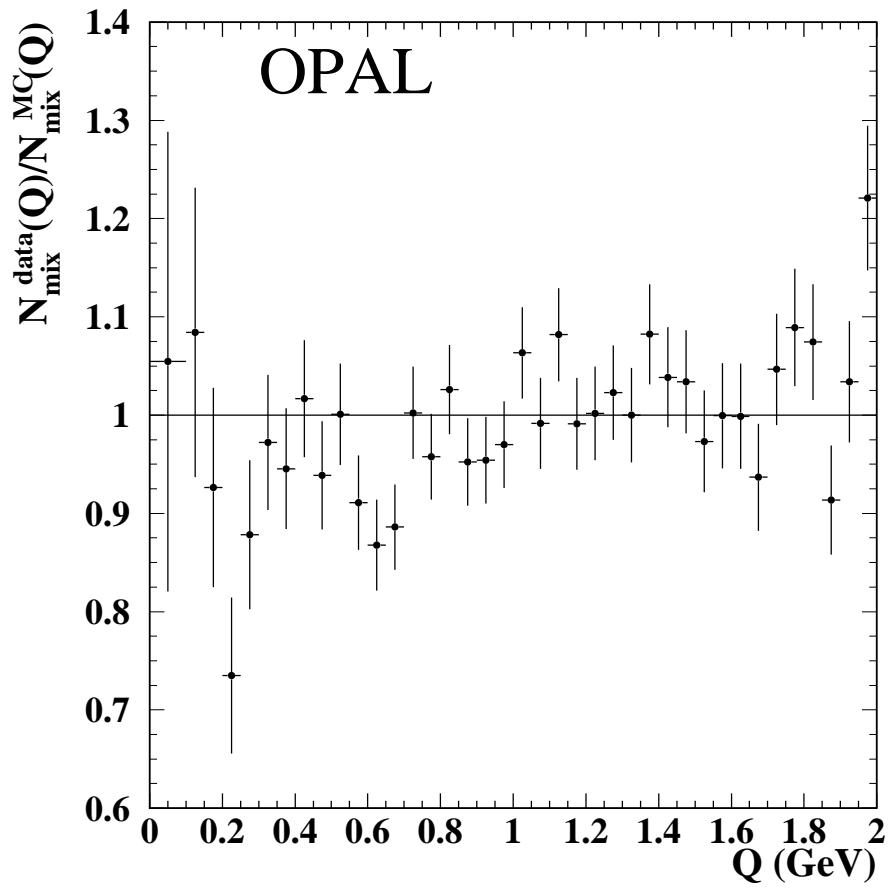


Figure 5: Comparison of the hemisphere-mixed Q distributions in the data and the Monte Carlo using the ratio $N_{mix}^{data}(Q)/N_{mix}^{MC}(Q)$. The errors are statistical only.

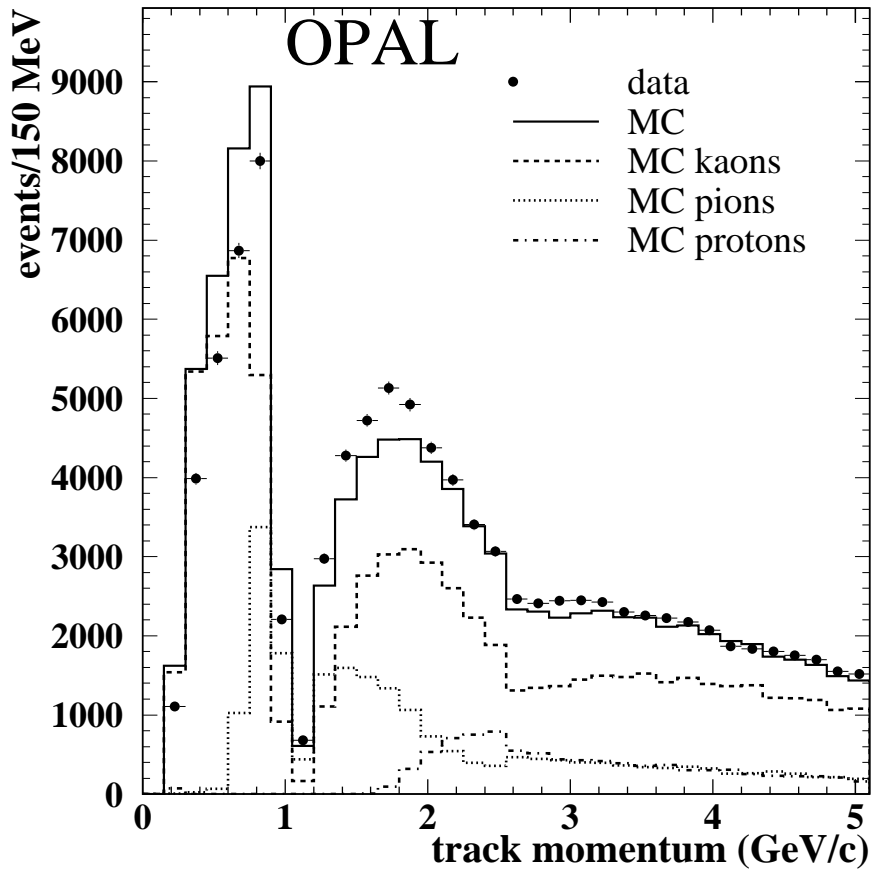


Figure 6: Momentum distribution of kaon candidates in the data and the Monte Carlo. The spectra for true kaons, pions and protons in the Monte Carlo are also shown.